

Visible Emission Bands of KXe_n Polyatomic ExciplexesT. Yabuzaki,^(a) A. C. Tam,^(b) S. M. Curry,^(c) and W. Happer*Columbia Radiation Laboratory, Physics Department, Columbia University, New York, New York 10027*

(Received 2 March 1978)

Intense green emission bands are observed when potassium vapor in several amagats of xenon is illuminated with the 4067-Å line of a krypton-ion laser. The very pronounced dependence of this green band on temperature and xenon density is consistent with the behavior expected for KXe_n exciplexes with n ranging from 1 to at least 4.

Radiative processes in dense gases have received considerable attention in the past few years. One of the motivations for the study of such systems has been the great success of excimer lasers in producing efficient, high-power visible and ultraviolet radiation. At sufficiently high gas pressures, excited atoms often react to form bound electronically excited states of rather improbable molecules (noble-gas fluorides¹ and alkali-noble-gas combinations²) which are dissociative in the ground electronic states. These "exciplex" molecules are often good laser species since the ground states self-destruct by dissociation and do not accumulate in sufficient numbers to reabsorb the laser light.

In this Letter we report on our observations of an unusual class of polyatomic exciplexes, KXe_n (58) molecules, which can be thought of as cluster ions KXe_n^+ , with $n = 1, 2, 3, \dots$, and a rather extended valence electron in an orbit which resembles the first excited S state ($5S$) of the potassium atom.

We produce these exciplex molecules by exciting a glass cell containing saturated potassium vapor in high-density xenon gas with the 4067-Å line of a krypton-ion laser. This laser line, which has a power of 140 mW, excites the pressure-broadened red wing of the (4044/4047)-Å second resonance line of potassium. The fluorescence from the cell is observed with a monochromator. The entire visible region of the spectrum is dominated by an intense green emission band. The most striking features of this band are illustrated in Fig. 1. The band consists of two parts, a well-defined symmetrical peak centered near 5220 Å, which is known³ to be an emission band of potassium monoxenide $KXe(5S) \rightarrow KXe(4S)$, and a broad asymmetric emission band between 5300 and 7000 Å which we attribute to the superposed emission bands of polyatomic exciplexes: $KXe_n(5S) \rightarrow KXe_n(4S)$ with $n = 2, 3, 4, \dots$. We shall henceforth refer to these bands as the monoxenide and polyxenide bands, respectively.

This system is particularly convenient for quantitative study since the narrow monoxenide emis-

sion peak remains well defined over a broad range of temperature and xenon densities and it can be used as a reference of intensity for the polyxenide band.

From data such as that shown in Fig. 1, several important properties of the polyxenide band can be recognized:

- (1) The polyxenide band narrows substantially at higher temperatures. The monoxenide band, in contrast, broadens slightly with increasing temperature.
- (2) The polyxenide band broadens substantially with increasing xenon density. The monoxenide band width is comparatively much less affected by xenon density.
- (3) The peak of the polyxenide band shifts substantially toward longer wavelengths for decreasing temperature.

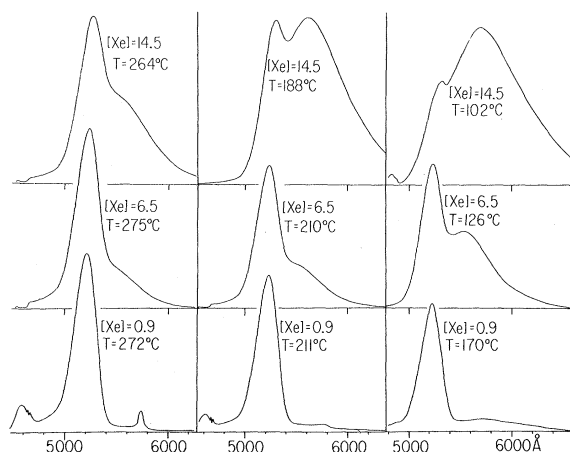


FIG. 1. Fluorescence spectra of potassium monoxenide and polyxenide at various cell temperatures and xenon densities (given in amagats). At low xenon density (lower curves), the monoxenide component is dominant. The small peaks observed near 4600 and 5750 Å for $[Xe] = 0.9$ amagat are due to alkali dimer fluorescence, since they are also observed in the absence of xenon. At high xenon density, the relative intensity of the red-shifted polyxenide component becomes progressively greater as the temperature is reduced.

The dependence of the polyxenide band on temperature and xenon density can be seen with particular clarity by using the monoxenide band as a reference of intensity. We define the relative intensity $S(\lambda, [\text{Xe}], T)$ of the polyxenide band to the monoxenide band by

$$S(\lambda, [\text{Xe}], T) = \frac{I(\lambda, [\text{Xe}], T) - \alpha I(\lambda, [\text{Xe}]_0, T)}{\alpha I(\lambda_0, [\text{Xe}]_0, T)}, \quad (1)$$

where λ_0 is the wavelength of the peak of the monoxenide band, and the constant α is defined by

$$\frac{I(\lambda, [\text{Xe}], T)}{I(\lambda, [\text{Xe}]_0, T)} = \alpha \text{ for } \lambda < 5220 \text{ \AA}. \quad (2)$$

Here $I(\lambda, [\text{Xe}]_0, T)$ is defined as the fluorescence spectrum at low xenon densities, when only the monoxenide spectrum is present. We have found that the polyxenide spectrum is negligible at $[\text{Xe}] \approx 0.9$ amagat, and so we can take $I(\lambda, [\text{Xe}]_0, T)$ as the fluorescence spectrum at $[\text{Xe}] \approx 0.9$ amagat.

The relative intensity S at a xenon density of 8.4 amagats is shown in Fig. 2(a). The temperature dependence of the relative intensity was found to be given by

$$S(\lambda, [\text{Xe}], T) = W(\lambda, [\text{Xe}]) \exp[E(\lambda)/kT]. \quad (3)$$

Some typical plots of $\ln S(\lambda, [\text{Xe}], T)$ versus $1/T$ are shown in Fig. 2(b). The slopes of the straight

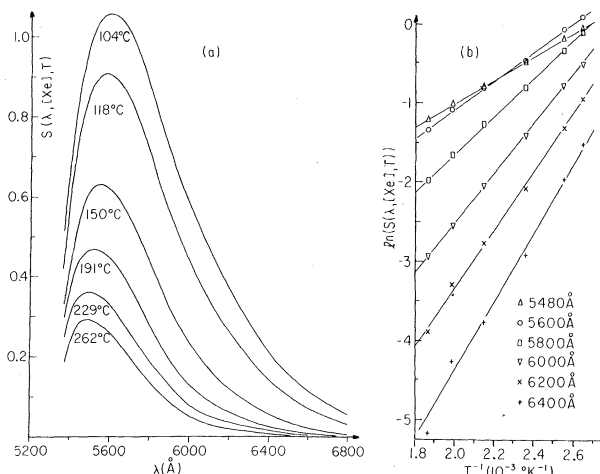


FIG. 2. (a) Spectra of the polyxenide component at a xenon density of 8.4 amagats, measured at various temperatures. The polyxenide spectra are obtained by subtracting the monoxenide component from the original data and then normalizing to the amplitude of the monoxenide peak. (b) The logarithm of the polyxenide component is shown plotted against the reciprocal of the absolute temperature for several different fluorescence wavelengths.

lines in Fig. 2(b) are proportional to the energies $E(\lambda)$. We have made plots similar to those of Fig. 2 for xenon densities of 11.4, 8.4, 8.1, 6.6, 6.4, 5.4, and 4.0 amagats. We find that the energies $E(\lambda)$ are independent of the xenon density to within our experimental accuracy of $\pm 5\%$, and they can be well represented by the empirical formula

$$E(\lambda) = 2.125\lambda - 10675, \quad (4)$$

with $E(\lambda)$ in cm^{-1} and λ in the range of 5400–6400 Å.

Our measurements of xenon density are probably in error by $\pm 10\%$ because of the cell preparation procedure, which consists of freezing xenon at a known initial temperature, pressure, and volume into a small glass cell of known volume. To within the uncertainties of the xenon-density determination, the constants of proportionality $W(\lambda, [\text{Xe}])$ of Eq. (3) have a power-law dependence on the xenon density,

$$W(\lambda, [\text{Xe}]) = [\text{Xe}]^{n(\lambda)-1} G(\lambda), \quad (5)$$

where the exponent $n(\lambda) - 1$ depends strongly on wavelength and can be represented by the empirical formula

$$n(\lambda) - 1 = 1.74 \times 10^{-3} \lambda - 8.23 \quad (6)$$

with λ in angstroms.

Finally the line shape factor $G(\lambda)$, which is independent of temperature and xenon density over the range of our experimental investigations, $110^\circ\text{C} \leq T \leq 300^\circ\text{C}$ and $1 \text{ amagat} \leq [\text{Xe}] \leq 12 \text{ amagats}$, is given by the empirical formula

$$G(\lambda) = 1778.5 - 0.668\lambda + 6.28 \times 10^{-5} \lambda^2. \quad (7)$$

In summary we have found that over a rather large range temperature and xenon density the polyxenide emission band is represented by the formula

$$S(\lambda, [\text{Xe}], T) = G(\lambda) [\text{Xe}]^{n(\lambda)-1} \exp[E(\lambda)/kT]. \quad (8)$$

The parameters, $E(\lambda)$, $n(\lambda)$, and $G(\lambda)$ are plotted in Fig. 3.

Because nothing is yet known about the potential surfaces for polyxenide molecules we cannot give a detailed theoretical analysis of the experimental data. However, we can assign a plausible physical meaning to the empirically determined parameters of (8). We may assume that each polyxenide species KXe_n has a characteristic emission band, similar to but broader than the

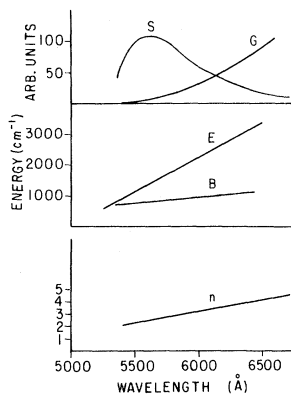


FIG. 3. Experimentally determined empirical functions $n(\lambda)$, $E(\lambda)$, and $G(\lambda)$. The function $B(\lambda)$, representing the binding energy per xenon atom, and a typical polyxenide line shape $S(\lambda)$ are also shown.

monoxenide band, for integral values of n ($n = 2, 3, 4, \dots$). The peaks of the emission bands of KXe_n shift systematically to longer wavelengths for increasing values of n . A large part of the red shift is due to the binding energy of Xe atoms to K(5S). The polyxenide bands of Fig. 2 therefore consist of the superposed and unresolved emission bands of KXe_2 , KXe_3 , KXe_4 , etc. Collisional rates are very fast in the high density systems we are studying (two-body collision rate is $\sim 10^{10} \text{ sec}^{-1}$, and three-body collision rate is $\sim 10^8$ to 10^9 sec^{-1} for a xenon density of 10^{20} cm^{-3}). The radiative decay rate of K(5S) is comparatively slow ($2 \times 10^7 \text{ sec}^{-1}$). Hence we expect to have thermal equilibrium among the various species K(5S), $KXe(5S)$, and $KXe_n(5S)$ for n being 2, 3, \dots . Therefore we expect the intensity of the emission band due to KXe_n to be proportional to $[Xe]^n$. Since there is substantial overlap of these bands the apparent density dependence of the fluorescence of wavelength λ is $[Xe]^{n(\lambda)}$ where $n(\lambda)$ is the measured noninteger exponent represented by the empirical formula (6). In this interpretation the exponent $n(\lambda)$ is the average number of xenon atoms attached to a potassium atom when the fluorescent wavelength is λ . The values λ_p defined by $n(\lambda_p) = p$ with $p = 2, 3, 4$, etc., can be identified approximately as the peak wavelengths of the emission bands of KXe_2 , KXe_3 , KXe_4 , etc. From Fig. 3 we see that $\lambda_2 = 5500$, $\lambda_3 = 5900$, and $\lambda_4 = 6400 \text{ \AA}$. The peak of the well-resolved monoxenide spectrum occurs at $\lambda_1 = 5220 \text{ \AA}$.

The energy $E(\lambda)$ can be thought of as the internal energy (not enthalpy because of our conditions

of constant density rather than constant pressure) released in the reaction



We may define a quantity $B(\lambda)$ by

$$B(\lambda) = E(\lambda) / [n(\lambda) - 1], \quad (10)$$

and we shall call $B(\lambda)$ the mean binding energy per xenon atom attached to the $KXe(5S)$. This mean binding energy is only approximately equal to the mean energy required to detach a xenon atom from the polyatomic molecule (the two energies differ by a quantity of the order of kT). Figure 3 shows a plot of $B(\lambda)$, which is of the order of 100 cm^{-1} per xenon, and it increases slightly as more xenons are added. In our experiment, the thermal energy $kT \sim 300 \text{ cm}^{-1}$, and so any given Xe atom in the cluster has a probability of only 0.1 to be moving fast enough to escape from the cluster.

The line-shape factor $G(\lambda)$ is perhaps the most remarkable property of the polyxenide band. The function $G(\lambda)$ is proportional to a factor which measures the statistical weight of the configurations of potassium polyxenide molecules which radiate at λ , and a mean transition rate of the configurations. Since the statistical weight factor decreases with increasing n , the rapid growth of $G(\lambda)$ with increasing λ must be due to an increase in the decay rate with λ . Indeed we expect a substantial increase in the radiative transition rate with λ , that is, with the number of attached xenon atoms, because both the monoxenide and polyxenide emission bands of Fig. 1 correlate with a highly forbidden electronic transition of the free atom K(5S)–K(4S). Each additional xenon atom in $KXe_n(5S)$ will cause further mixing of the electronic wave functions of the free potassium atom, and the radiative transition will therefore become increasingly more allowed as more xenons are attached. The unprecedented prominence of the green potassium polyxenide band is due to the fact that it originates from a forbidden electronic transition of the free potassium atom. This seems to be one of the main reasons that multiple-perturber effects are so much more striking in the data presented in this paper than in the pressure-broadened resonance lines of the alkali atoms.⁴ Since the first excited P states of free alkali atoms have fully allowed transition rates to the ground state, they can only be weakened by multiple-perturber effects, while forbidden lines are strongly enhanced.

The nature of these polyxenide exciplexes is

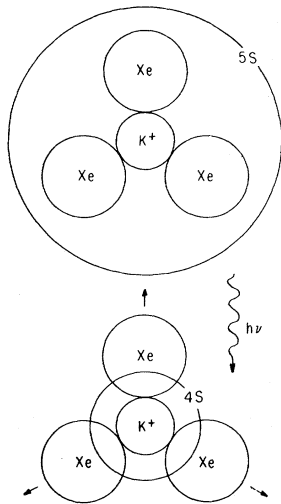


FIG. 4. Schematic representation of the physical dimensions of potassium polyxenide molecules. The ionic core of K^+ has a radius of $2.5a_B$ ($a_B = \text{Bohr radius}$) and a xenon atom has a radius, $3.6a_B$. For the 5S state of potassium the mean radius of the electron charge distribution is $11.8a_B$, so that the xenon atoms are primarily affected by the polarizing influence of the ionic core. After a transition to the ground state, the electronic mean radius is only $4.7a_B$, and the Xe atoms are no longer bound.

still uncertain, but it is interesting to note that cluster ions of the form $K^+(H_2O)_n$ have been extensively studied,⁵⁻⁶ and six or more waters of hydration are observed by mass-spectroscopic techniques. Similar bonding of alkali ions to other neutral molecules (O_2 , N_2 , and CO_2) has been observed⁷ and calculated theoretically.⁸ The highly polarizable noble gas xenon ($\alpha = 4 \text{ \AA}^3$) can be expected to form analogous cluster ions K^+Xe_n , and an electron could bind to such a cluster ion to form the initial and final states of the polyxenide transitions reported in this paper. A

sketch to indicate the dimensions of such a system is shown in Fig. 4.

We thank George Moe for many useful suggestions. This research was supported by the U. S. Army Research Office (Durham) under Contract No. DAAG29-77-G-0015 and the Joint Services Electronics Program under Contract No. DAAG29-77-C-0019, and by the National Science Foundation under Grant No. NSF ENG 76-16424. One of us (S.M.C.) acknowledges the receipt of a fellowship from the Alfred P. Sloan Foundation.

^(a)On leave from the Ionosphere Research Laboratory, Kyoto University, Kyoto, Japan.

^(b)Present address: Bell Telephone Laboratories, Murray Hill, N. J. 07974.

^(c)On leave from the University of Texas at Dallas, P. O. Box 688, Richardson, Texas 75080.

¹See, for example, M. Rokni, J. H. Jacob, J. A. Mangano, and R. Brochu, *Appl. Phys. Lett.* **32**, 223 (1978).

²See, for example, G. York, R. Schleps, and A. Gallagher, *J. Chem. Phys.* **63**, 1052 (1975); A. C. Tam, G. Moe, W. Park, and W. Happer, *Phys. Rev. Lett.* **35**, 85 (1975); G. Moe, A. C. Tam, and W. Happer, *Phys. Rev. A* **14**, 349 (1976); J. G. Eden, B. E. Cherrington, and J. G. Verdeyen, *IEEE J. Quantum Electron.* **12**, 698 (1976).

³A. C. Tam, G. Moe, B. R. Bulos, and W. Happer, *Opt. Commun.* **16**, 376 (1976).

⁴W. P. West, P. Shuker, and Alan Gallagher, *J. Chem. Phys.* **68**, 3864 (1978); W. P. West and A. Gallagher, *Phys. Rev. A* **17**, 1431 (1978).

⁵I. Dzidic and P. Kebarle, *J. Phys. Chem.* **74**, 1466 (1970).

⁶K. G. Spears and S. H. Kim, *J. Phys. Chem.* **80**, 673 (1976).

⁷G. E. Keller and R. A. Beyer, *J. Geophys. Res.* **76**, 289 (1970), and *Trans. Am. Geophys. Union* **52**, 303 (1971).

⁸K. G. Spears, *J. Chem. Phys.* **57**, 1850 (1972).